Journal of Magnetic Resonance **148,** 327–337 (2001)
doi:10.1006/jmre.2000.2255, available online at http://www.idealibrary.com on IDEAL®

Spectral Editing in ^{13}C MAS NMR under Moderately Fast Spinning Conditions[1]

Enrico De Vita and Lucio Frydman[2]

Department of Chemistry (M/C 111), University of Illinois at Chicago, 845 W. Taylor Street, Chicago, Illinois 60607-7061

Received June 26, 2000; revised November 6, 2000

Novel procedures for the spectral assignment of peaks in high-resolution solid-state ^{13}C NMR are discussed and demonstrated. These methods are based on the observation that at moderate and already widely available rates of magic-angle spinning (10–14 kHz MAS), CH and CH_2 moieties behave to a large extent as if they were effectively isolated from the surrounding proton reservoir. Dipolar-based analogs of editing techniques that are commonly used in liquid-state NMR such as APT and INEPT can then be derived, while avoiding the need for periods of homonuclear ^1H–^1H multipulse decoupling. The resulting experiments end up being very simple, essentially tuning-free, and capable of establishing unambiguous distinctions among CH, CH_2, and $-\overset{|}{\underset{|}{C}}-/-CH_3$ carbon sites. The principles underlying such sequences were explored using both numerical calculations and experimental measurements, and once validated their editing applications were illustrated on a number of compounds. © 2001 Academic Press

Key Words: **solid-state NMR; magic-angle spinning; spectral assignment techniques; dipolar couplings; polarization transfer.**

1. INTRODUCTION

The advent of cross polarization (CP), magic-angle spinning (MAS), and efficient forms of proton decoupling has made the acquisition of ^{13}C solid-state NMR spectra with high sensitivity and high resolution routine (*1–5*). Nevertheless, whereas numerous techniques have been proposed to assign peaks in solution ^{13}C NMR spectra, mainly on the basis of heteronuclear *J* couplings (*6, 7*), these principles have not found a direct extrapolation to the case of solids. The search for methods that will facilitate the editing of high-resolution ^{13}C solid NMR spectra, particularly when dealing with complex biological or synthetic systems, consequently remains a topic of active research (*8–24*). Broadly speaking, the methods that have been pursued in this area can be divided into two categories: those that rely on scalar C–H *J* interactions in order to differentiate among CH_n groups and those that operate on the basis of heteronuclear dipolar couplings. The former were demonstrated early on and, based largely on modified solution dephasing techniques, shown to be particularly efficient when dipolar couplings are substantially reduced by molecular motions (*10–12*). More recently Lesage *et al.* have shown that, using highly efficient homonuclear ^1H–^1H decoupling and heteronuclear MAS averaging, such *J*-based strategies could also be extended to ordinary rigid solids (*20, 22*).

Spectral editing alternatives have also relied on the use of dipolar couplings. Particularly important among these techniques is the dipolar-dephasing experiment, which easily differentiates resonances of nonprotonated and methyl carbons from those of CH and CH_2 by introducing a short interval without ^1H decoupling prior to the signal's acquisition (*3, 8, 9*). The first group of sites can be further distinguished by their different chemical shift parameters, yet differentiating methine from methylene groups by this approach has remained an enduring challenge. Probably the most robust alternative hitherto available for achieving a methine/methylene distinction is the one exploiting the different rates of ^{13}C cross-polarization/depolarization from and to protons in these moieties (*16–19, 23, 24*). Although widely applicable, such editing protocols still require a precalibration based on model compounds in order to account for the peculiarities of each particular experimental setup. Methods have also been proposed for discriminating between CH and CH_2 groups based on the differences shown by their heteronuclear local field spectra (*13–15, 21*). Such approaches have been demonstrated in both uni- and bidimensional versions, and although promising, their routine use did not become widespread. This is probably a combined result of the slight differences between the groups' heteronuclear couplings and of the need to achieve a proper isolation of these groups via efficient homonuclear ^1H–^1H decoupling.

It has recently been shown that a very nearly ideal short-term heteronuclear local field evolution can actually be achieved in the absence of multiple-pulse homonuclear decoupling (*25*), simply by carrying out unassisted MAS at moderately fast spinning rates ($\omega_r/2\pi \geq 10$ kHz). This paper further explores

[1] Presented in part at the 41st Rocky Mountain Conference, Denver, CO, August 1999; Poster 298.

[2] To whom correspondence should be addressed at Department of Chemistry (M/C 111), University of Illinois at Chicago, 845 W. Taylor Street, Room 4500, Chicago, IL 60607-7061. Fax: (312) 996-0431. E-mail: lucio@samson.chem.uic.edu.

1090-7807/01 $35.00

this feature and discusses a number of alternatives that enable its use to achieve a simple and clear differentiation among C/CH_3, CH, and CH_2 groups based on the different local field behavior of the ^{13}C spins. The methods that are thus derived are again based on differences in the heteronuclear dipolar evolutions characterizing these groups, but unlike previous techniques they do not require multiple-pulse or CP precalibrations. They do, however, require controlling the relative ratio between the effective ^{13}C–^{1}H dipolar coupling ω_{CH} and the spinning rate, a manipulation that, as is here demonstrated, can be simply implemented with the aid of a few π pulses. The novel forms of spectral editing that follow from these considerations are illustrated on a variety of natural-abundance organic compounds.

2. EXPERIMENTAL AND NUMERICAL METHODS

All experiments in this study were performed at room temperature and a 7.1-T laboratory-built NMR spectrometer. This instrument was controlled by a Tecmag, Inc., acquisition system and used a laboratory-built doubly tuned probe equipped with a 3.2-mm Chemagnetics MAS spinning unit. For carrying out the measurements rotors were packed with between 10 and 15 mg of sample. All chemicals were purchased from Sigma at natural isotopic abundance and used without further purification with the exception of vitamin B_{12}, which was recrystallized from ethanol before investigation. In all experiments continuous wave decoupling with a field strength $\omega_{RF}/2\pi \approx$ 150 kHz was applied to the protons during the ^{13}C signal acquisition period. When necessary, CP with an RF strength of about 100 kHz was applied on the proton channel, while a ramped RF field was applied at the ^{13}C frequency with its central amplitude matched to obtain an optimum signal (*1*, *26*). The duration of the π pulses required in some of the sequences described below was set at 3.5 μs for the ^{1}H and ^{13}C channels. Further details about the pulse sequences that were introduced are given in the corresponding paragraphs and figure legends.

Numerical spin evolution calculations were carried out in unison with the experiments in order to guide their design and monitor the relevance of the various parameters that are involved. All simulations were performed using custom-written C codes running on a HP 9000/800 mainframe computer, where they lasted from a few seconds to a few minutes. The systems typically considered were random powders of isolated ^{13}C–^{1}H or ^{1}H–^{13}C–^{1}H moieties, the latter with a H–C–H angle of 109.5°. For these simulations a "direct" method was used, which integrated the equation of motion for the full spin density matrix over the duration of the MAS NMR pulse sequence using sufficiently small time increments Δt. Calculations could account for heteronuclear ^{13}C–^{1}H and homonuclear ^{1}H–^{1}H dipolar coupling Hamiltonians, as well as for isotropic and anisotropic chemical shifts. Throughout these computations, RF pulses were considered ideal δ-functions and dipole–dipole interactions were neglected during periods of CW decoupling. With these considerations in mind the density matrix for each single crystallite was propagated as a function of the editing time t_1 and acquisition time t_2, and the resulting signals were subsequently integrated over $\approx 33^3$ (α, β, γ) powder orientations. In a majority of the plots illustrated below these signals are shown after Fourier transformation against t_2, that is at the frequency position of the isotropic ^{13}C peak being considered, with the indirect evolution time t_1 expressed as a fraction of the rotor period T_r. Finally, and as reported in the following paragraphs, the evolution of isolated CH and homonuclear-decoupled CH_2 groups could also be calculated by a simple powder integration of the analytical signal expressions, leading to results that were analogous to those of the complete numerical propagations but requiring much shorter computational times.

3. RESULTS

Local Field Spectroscopy without Homonuclear Decoupling

As mentioned, heteronuclear ^{13}C–^{1}H local field experiments can serve as useful starting points for solid-phase ^{13}C spectral editing: major differences exist between the dephasing rates of CH_3/C and other protonated carbon, while more subtle effects can be brought to bear in order to distinguish CHs from CH_2s. The latter usually require (i) homonuclear decoupling to ensure the isolation and ideal spin evolution within these groups and (ii) a choice of spinning rate that maximizes the contrast between the relatively similar ^{13}C–^{1}H dipolar evolutions exhibited by these two groups. In a recent investigation on the behavior of multispin systems subject to increasingly higher MAS rates, we have shown both numerically and experimentally that the need for homonuclear decoupling is lifted once sample spinning rates reach $\approx$10 kHz, provided that the ^{13}C signals are probed for relatively short periods of time (one to two rotor periods) (*25*). The apparent ω_{CH} couplings defining the local field evolution will then correctly reflect the internuclear C–H distance while being free from uncertainties related to multiple-pulse scaling factors and yield information that may be used in quantitative structural or dynamic determinations.

This feature could in principle be exploited toward the implementation of simple, multiple-pulse-free, spectral editing protocols. This, however, is complicated by the conflicting demands of having a nimble control on the ω_{CH}/ω_r ratio in order to better distinguish CHs from CH_2s, while at the same time keeping the spinning at rates $\omega_r \geq \omega_{CH}/2$ in order to allow for the neglect of the internuclear ^{1}H–^{1}H couplings. A solution to this conflict is offered by the 2*x* and 4*x* coupling amplification sequences recently described by Hong *et al.*, and which on the basis of a few additional π pulses allow one to double or quadruple the apparent dipolar coupling defining the heteronuclear MAS spin evolution (*27*, *28*). Such protocols, initially demonstrated in the presence of

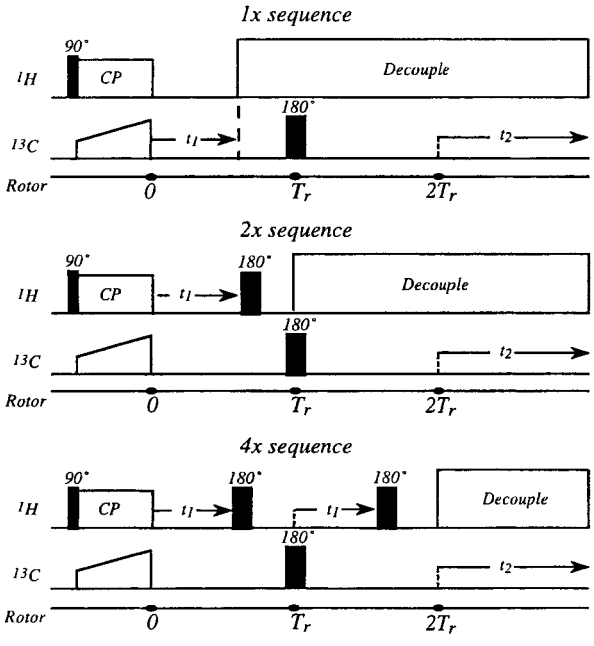

FIG. 1. Pulse sequences employed for the 1*x*, 2*x*, and 4*x* amplifications of the effective ^{13}C–^{1}H local fields in MAS NMR experiments.

^{1}H–^{1}H decoupling, were adopted for the present study in combination with unassisted MAS NMR. The resulting 1*x* free evolution local field pulse sequence, together with its 2*x* and 4*x* variants, is presented in Fig. 1. As described by Hong *et al.* in their original study, these sequences rely on the time reversal that π pulses can impart on the dipolar spin evolution if applied at time t_1 into the rotor period T_r (*28*). For instance, given a ^{13}C–^{1}H spin pair subject to a dipolar coupling ω_{CH} and spinning at a rate ω_r, the 2*x* sequence produces for each crystallite in the sample a dynamic evolution phase,

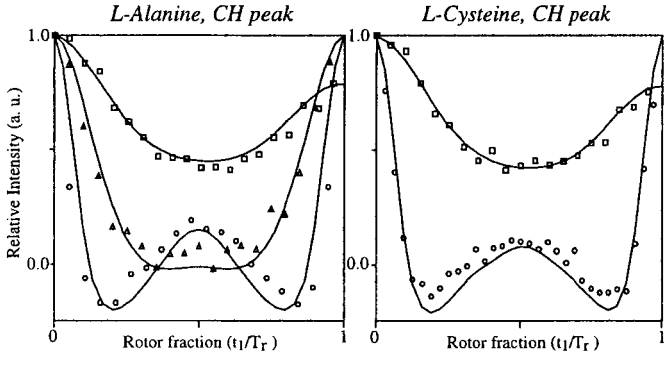

FIG. 2. Local field dephasing behavior displayed by methine peaks under the action of the 1*x* (□), 2*x* (△), and 4*x* (○) pulse sequences sketched in Fig. 1, for L-alanine and L-cysteine samples. The solid lines represent best fit simulations assuming isolated ^{13}C–^{1}H pairs and a $\omega_{CH}/2\pi = 22 \pm 1$ kHz (internuclear distance of 1.12 ± 0.01 Å). A 0.33-ms exponential decay was applied to the simulated 1*x* curves in order to account for the experimental relaxation. The actual relative *S*/*N* ratios shown by the various sequences were 1 (1*x*), 0.84 (2*x*), and 0.53 (4*x*).

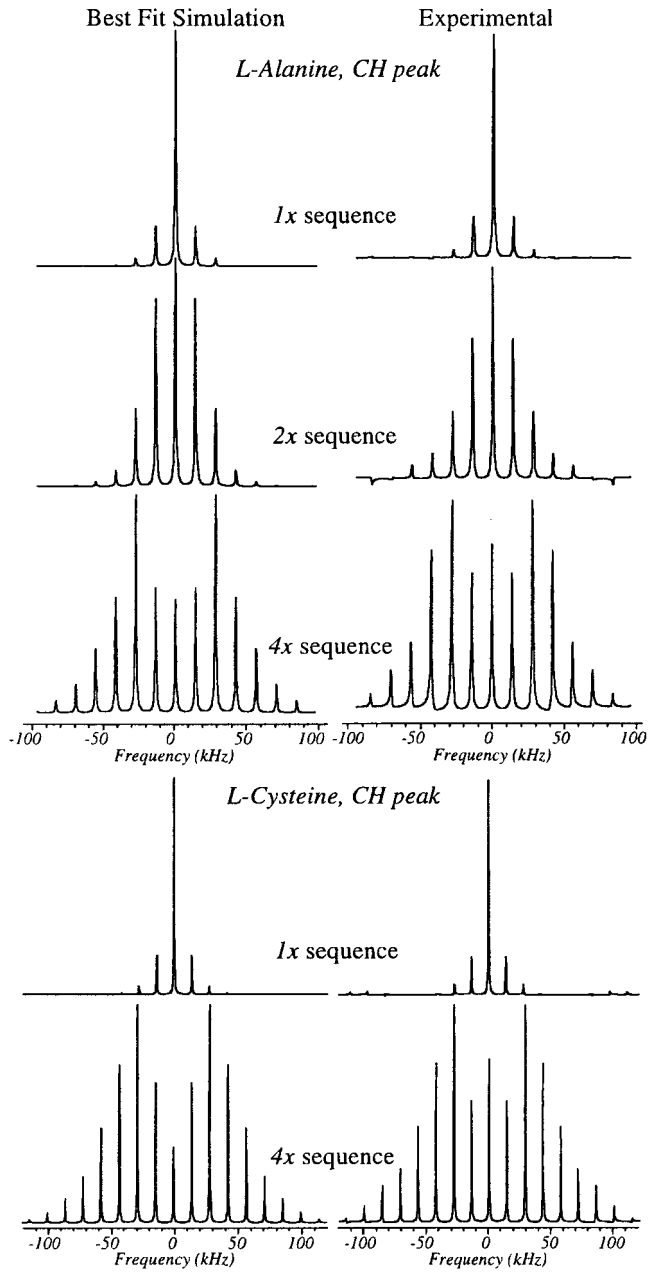

FIG. 3. Comparison between the experimental dipolar sideband patterns afforded by the CH groups in L-alanine and L-cysteine and their the best fit simulations. Experimental spectra were obtained from the dipolar dephasing curves displayed in Fig. 2 using a processing procedure similar to that described in Ref. (*25*). The unscaled ^{13}C–^{1}H dipolar coupling parameters used in the simulations were 21 kHz for L-alanine and 22 ± 0.5 kHz for L-cysteine.

$$\begin{aligned}\phi(\pi\ @\ t_1, \omega_{CH}, \omega_r) &= -2\phi(t_1, \omega_{CH}, \omega_r)\\ &= -\phi(t_1, 2\omega_{CH}, \omega_r)\\ &= -\phi(2t_1, \omega_{CH}, \omega_r/2). \qquad [1]\end{aligned}$$

In essence, this strategy allows one to mimic a situation where

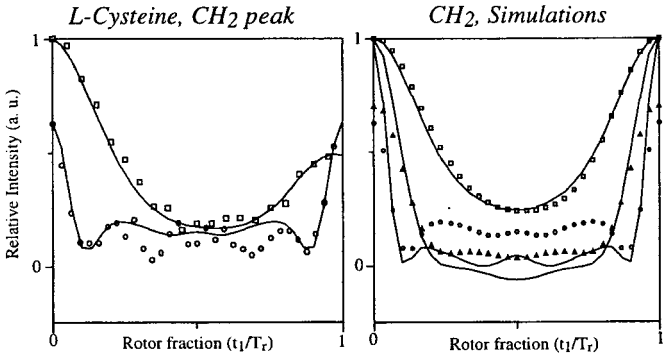

FIG. 4. Dipolar evolution behavior displayed by methylenes under the effects of the pulse sequences sketched in Fig 1. Left: Comparison between the experimental $1x$ (□) and $4x$ (○) dipolar dephasing data for L-cysteine and best fit simulations calculated for isolated ^{1}H–^{13}C–^{1}H systems with C–H distances of 1.14 Å and all mutual couplings active (solid lines). Right: Comparison between the theoretical dipolar evolution that can be expected for methylenes possessing homonuclear ^{1}H–^{1}H couplings under the action of $1x$ (□), $2x$ (△), and $4x$ (○) sequences and the dephasing that would result if intramoieity homonuclear interactions were neglected (solid lines).

the apparent dipolar coupling constant has been doubled or, conversely, where the effective spinning rate has been halved. To obtain a $4x$ amplification of ω_{CH} the spin evolution needs to be extended over two rotor cycles and π pulses applied at times t_1, T_r, and $t_1 + T_r$. Notice that the assumption of isolated ^{13}C–^{1}H heteronuclear spin pairs implies that π pulses can be applied on either ^{13}C or ^{1}H channels; the sequences in Fig. 1 exploit this feature and distribute the pulses so as to avoid potential complications that could arise from a net isotropic or anisotropic ^{13}C chemical shift evolution.

Figure 2 illustrates the heteronuclear local field evolutions that were observed using these $1x$, $2x$, and $4x$ sequences over a single rotor period $0 \leq t_1 \leq T_r$ for the methine moieties of L-alanine and L-cysteine polycrystalline samples spinning at 14 kHz. Also shown for comparison are the dephasing curves that can be expected from the ideal operation of these sequences on a ^{13}C–^{1}H two-spin system characterized by a coupling ω_{CH} that best fitted the experimental data. The overall agreement between the experimental behavior and the two-spin expectations is very good. Besides an obvious amplification of the effective ω_{CH} coupling constants, the $2x$ and $4x$ experimental data also differ from their $1x$ counterparts in a somewhat smaller overall intensity (resulting from increasingly longer periods without ^{1}H decoupling) and in having equal signal magnitudes at $t_1 = 0$ and $t_1 = T_r$ (a result of their constant-time nature). Figure 3 compares the local field MAS NMR spectra that can be obtained from these experimental dephasing curves against ideal spectra calculated on the basis of CH pairs whose effective coupling constants have been doubled or quadrupled. Again, the overall agreement between experiment and expectation is very good. It is worth noticing that, although the number of significant sidebands in the $2x$ and $4x$ experiments is larger than in the $1x$ spectrum, an analysis of whether the former will yield a more reliable coupling information under these spinning conditions involves several additional considerations and is therefore far from trivial (*29*).

Also worth investigating is the behavior displayed by methylene groups when acted upon by these sequences. At stake here is the question of to what extent one needs to consider the ^{1}H–^{1}H intramoiety coupling when trying to properly describe the ^{13}C local field MAS evolution of this group. Toward this end Fig. 4 presents the experimental behavior observed for L-cysteine's methylene site and the results expected if the various pulse sequences were applied on CH_2 groups that are free from or subject to homonuclear ^{1}H–^{1}H interactions. As can be appreciated from the right-hand simulations in Fig. 4, the best quantitative agreement between the two sets of simulations is actually observed for the conventional $1x$ sequence, whereas for the $2x$ and $4x$ sequences the model based solely on heteronuclear couplings predicts a slightly more pronounced dephasing than its more realistic ^{1}H–^{1}H coupled counterpart. These differences, however, are minor, and at these fast spinning rates neither model deviates substantially from the behavior that is observed experimentally.

For the sake of completion, Fig. 5 presents the experimental dipolar dephasing behavior that is observed over one rotor period with the $1x$, $2x$, and $4x$ local field sequences for the nonprotonated and methyl carbon sites of the alanine and cysteine samples. Also shown in the figure are the best fits of these curves to the dephasing behavior expected for a ^{13}C site coupled to a single ^{1}H. When compared with the previous methine and methylene curves, such carbon sites are evidently characterized by weaker ω_{CH} coupling constants. Notably, these effective couplings are not identical, with the $-CH_3$ group showing a stronger coupling than its carbonyl counterparts. If these differences were to prove sufficiently general they could be used for distinguishing C and CH_3 groups on the basis of their respective heteronuclear local fields.

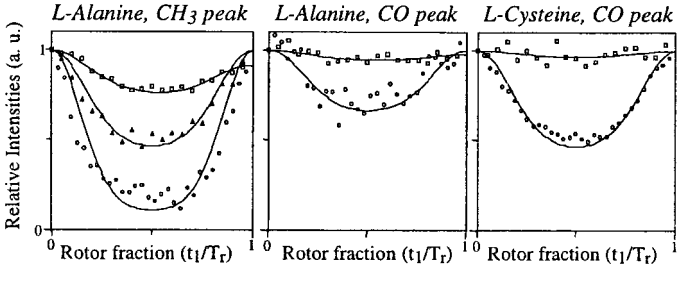

FIG. 5. Dipolar dephasing curves observed for the methyl group of L-alanine and for the carbonyl groups of L-alanine and L-cysteine as function of dephasing time and for the various pulse sequences sketched in Fig. 1: (□) $1x$, (△) $2x$, (○) $4x$. The solid lines represent the best fit curves assuming isolated C–H pairs and a simple $1x$ dephasing experiment. The ^{13}C–^{1}H couplings assumed in the various CH_3 simulations were $\omega_{CH}/2\pi = 10$, 22, and 36 kHz, respectively; the couplings used for the L-alanine CO simulations were 5.6 and 17, and those for the L-cysteine CO were 5.5 and 22 kHz.

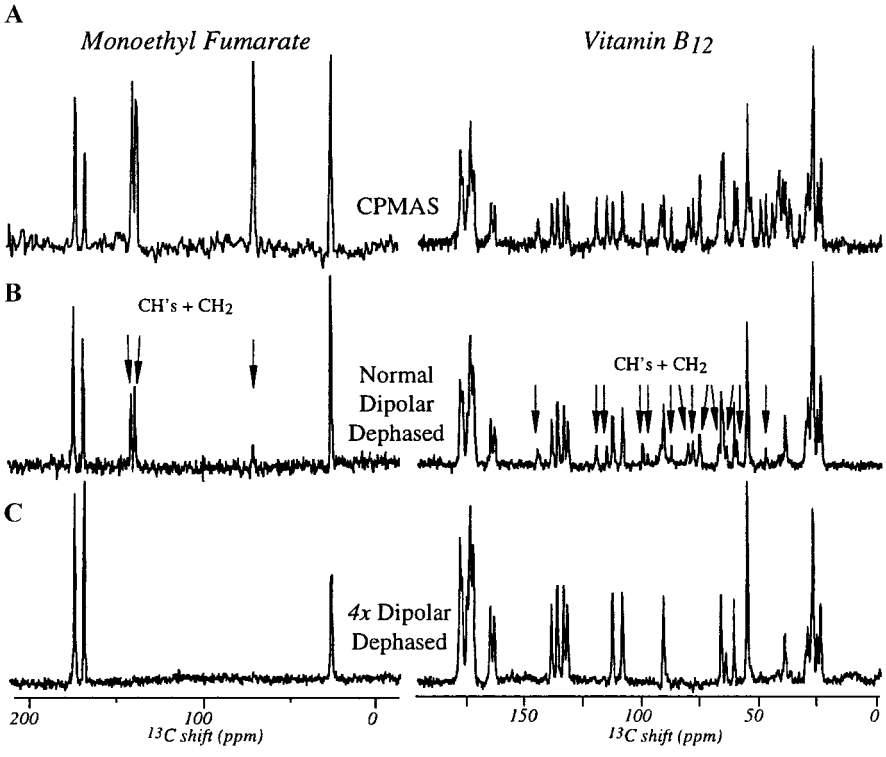

FIG. 6. Comparisons among the CPMAS, standard dipolar-dephased, and 4*x* dipolar-dephased spectra observed for monoethyl fumarate and for vitamin B_{12} samples spinning at $\omega_r/2\pi = 12$ kHz. The number of scans used in the various experiments were 32, 64, and 768 for the monoethyl fumarate, and 2048, 4096, and 12288 for vitamin B_{12}.

Spectral Editing via Dipolar Dephasing

For the purpose of dipolar-based editing, the main spectroscopic conclusions that follow from the previous paragraph are that at MAS rates $\omega_r/2\pi \geq 10$ kHz a reliable heteronuclear ^{1}H–^{13}C local field evolution can be retrieved without homonuclear ^{1}H–^{1}H decoupling and that, if so desired, the apparent strength of the ω_{CH} heteronuclear coupling can be doubled or quadrupled using simple experimental strategies.[3] Conversely, if instead of acting as a coupling amplification these sequences are viewed as dividing the effective spinning rates by factors of 2 or 4, these principles imply that effective spinning rates as low as 2.5 kHz can be imposed on the evolution of isolated CH, CH_2 systems in a simple manner. As an illustration of the applications that these principles may have on spectral editing, consider the conventional dipolar dephasing experiment, which by introducing a short period of interrupted decoupling prior to acquisition helps identify CH/CH_2 resonances (*9*). As spinning rates are increased the dephasing and ensuing suppression of these resonances stop being complete; this can be appreciated, for example, from the 1*x* curves shown in Figs. 2 and 4 for the free dipolar evolution of model ^{13}C–^{1}H and ^{13}C–$^1H_2$ systems. Further calculations reveal that even at the point of maximum ^{13}C–^{1}H dipolar dephasing, corresponding at moderate MAS rates to a rotor fraction of $t_1/T_r = 0.5$, interrupted decoupling stops being a clear assignment technique when the ω_{CH}/ω_r ratio drops below 2–3. These considerations are validated by the experimental results in Fig. 6, which show how dipolar-dephased spectra become contaminated with considerable CH_2- and CH-derived "cross-talk" when acquired at rates exceeding 12 kHz. By contrast, a much cleaner editing results if, under the same sample spinning conditions, couplings are amplified by factors of 2 or 4 prior to the acquisition; the bottom row of Fig. 6, for instance, illustrates how a properly tuned 4*x* dipolar dephasing experiment (sequence in Fig. 1 with $t_1 = 0.4\ T_r$) yields solely nonprotonated and methyl carbons with a selectivity comparable to that observed under slower spinning conditions.

As mentioned, the minor yet noticeable differences revealed by the heteronuclear ^{13}C dephasing curves of methines and methylenes can be exploited for distinguishing the resonances of these two groups. These dipolar-based analogs of the attached proton test (APT) experiment were thus explored a decade ago by Sethi, who demonstrated that in the absence of homonuclear interactions a distinction between CH and CH_2 groups would result if the effective ω_{CH}/ω_r ratio were set at

[3] Numerical simulations reveal that a nearly continuous scaling of the apparent ω_{CH}/ω_r ratio can actually be implemented with this type of sequences, by replacing the π pulse manipulations with shorter pulse angles.

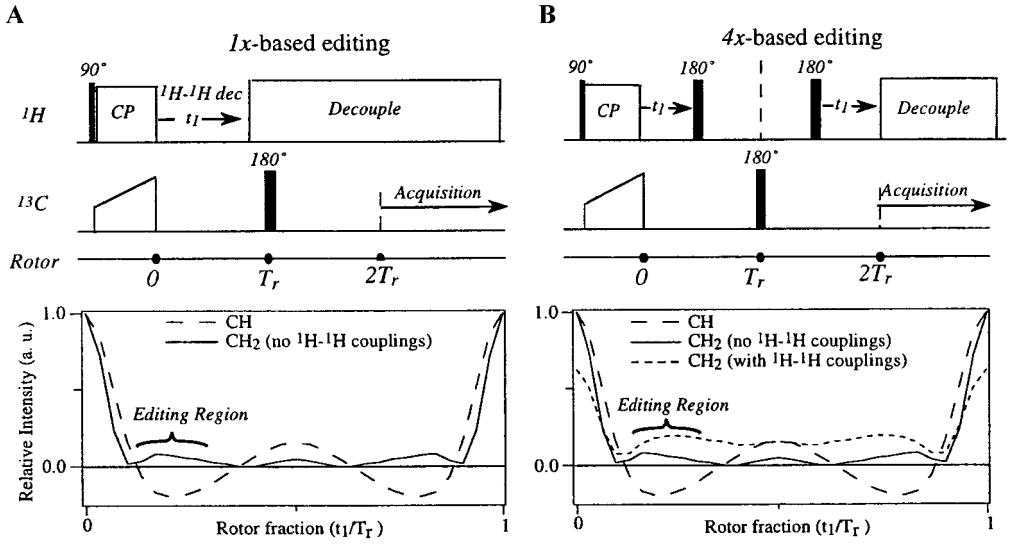

FIG. 7. Comparison between (A) the spectral editing pulse sequence proposed by Sethi (*15*) on the basis of MAS at 2 kHz and homonuclear ^{1}H–^{1}H decoupling and (B) a 4*x* dipolar editing sequence applied under fast MAS (curves calculated for $\omega_r/2\pi$ = 14 kHz). Shown underneath each sequence are the corresponding dipolar dephasing curves calculated for isolated methine and methylene groups; both approaches can differentiate CH from CH_2 moieties when $t_1/T_r \approx 0.25$ on the basis of the peaks' opposite phases.

approximately 6 (*15*). The rationale underlying this approach can be appreciated from the ideal dipolar dephasing plots in Fig. 7A, which show how under such conditions a dephasing period $t_1 \approx 0.2\ T_r$ will lead to a small positive methylene signal ($\approx +0.1$ of its initial amplitude) and to a larger negative methine peak (amplitude ≈ -0.2). The same study corroborated such predictions with the aid of relatively slow MAS rates ($\omega_r/2\pi \approx 2$ kHz) and of a BLEW-12 multiple-pulse homonuclear decoupling sequence which scaled ω_{CH} by a factor of $\approx$0.58. The considerations of the previous paragraph allow one to extend this type of editing to faster spinning conditions, while at the same time lifting the need for multiple-

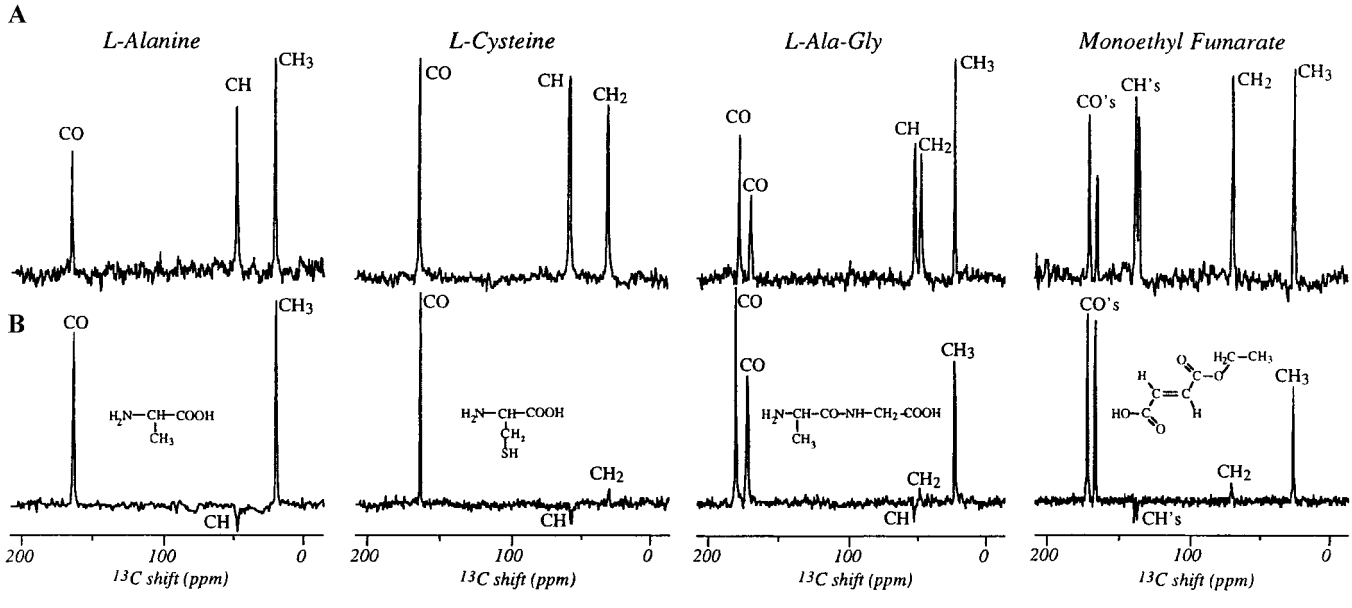

FIG. 8. Comparison between the (A) CPMAS and (B) 4*x* dipolar-edited spectra obtained applying the pulse sequence shown in Fig. 7B to a number of common organic compounds. A distinction is possible between the positive methylene signals and the negative ones from methines. All 4*x* spectra were acquired using 10 times as many scans as their conventional counterparts. Data for L-alanine and L-cysteine were acquired at $\omega_r/2\pi$ = 14 kHz, while L-ala-gly and monoethyl fumarate data were acquired at 12 kHz.

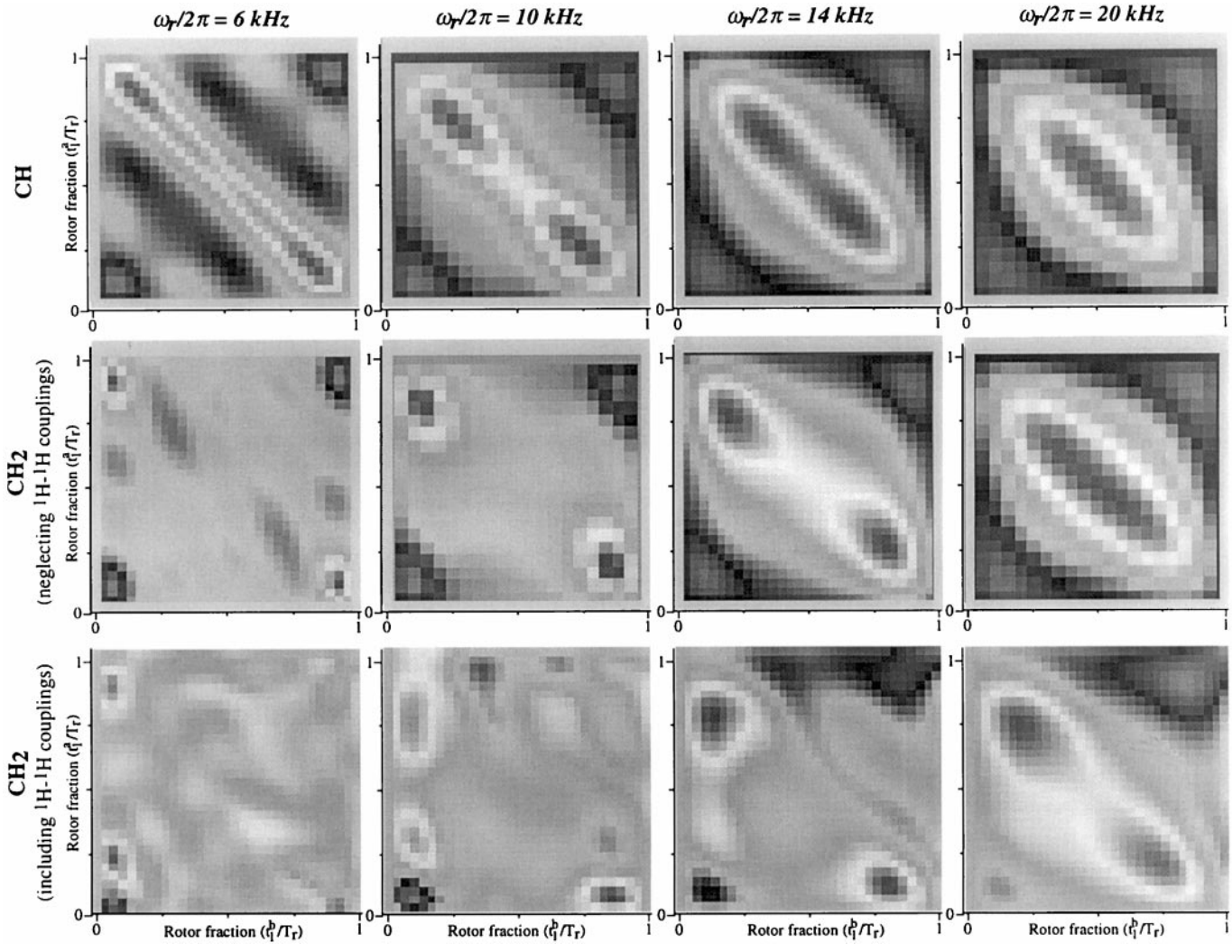

FIG. 9. $S(t_1^a, t_1^b)$ maps calculated for a solid-state INEPT transfer sequence (Eq. [2]) at four different MAS speeds. The top row shows the CH signal transfer map, the center row shows the signal transfer for a CH_2 group where ^{1}H–^{1}H dipolar couplings have been neglected, and the bottom row illustrates the transfer for a CH_2 system whose homonuclear ^{1}H–^{1}H interactions are taken into account. Notice that the gray scales refer only to absolute intensities within the map, with the darkest shades indicating a larger deviation from null. ^{13}C signals are positive along the $t_1^a + t_1^b = T_r$ anti-diagonal, with absolute maxima occurring toward $t_1^a = t_1^b = T_r/2$ at the highest spinning speeds. Negative values occur along the $t_1^a = t_1^b$ diagonal for values of t_1^a and t_1^b close to zero or T_r.

pulse ^{1}H–^{1}H decoupling. Indeed, given the usual range of static heteronuclear couplings in CHs and CH_2s (21–24 kHz) and the spinning rates required for effectively isolating these groups (10–14 kHz), it follows that a 4*x* amplification of the heteronuclear couplings will bring about the correct $\langle \omega_{CH}/\omega_r \rangle_{eff} \approx 6$ ratio required by this form of APT editing. This premise is supported by ^{13}C dephasing curves calculated under such conditions for CH and CH_2 groups (Fig. 7B). Notice that for the latter moieties, the main effect resulting from including an intraresidue ^{1}H–^{1}H coupling is a minor attenuation in the overall extent of the ^{13}C dephasing, which in terms of editing further helps to discriminate their signals from the negative methine peaks. From a practical standpoint several experiments were assayed to test these predictions (Fig. 8); they all gave the expected editing results without requiring any real "tuning" to speak of.

Spectral Editing via Coherent Polarization Transfer

Although conceptually and technically simple, the APT discrimination between CH and CH_2 groups that was just described suffers from two basic drawbacks which are already evident in the dephasing plots presented in Fig. 7. One is the largely attenuated signals with which the method operates ($\approx$10–20% when $t_1/T_r \approx 0.2$) and which in turn explain the order-of-magnitude increase that is required in the number of scans to match the signal-to-noise ratio observed using conventional CP. The second (and related) drawback arises from

the relative similarity between the dephasing curves of the two groups. As a result of this, even minor variations in the strengths of the ^{13}C–^{1}H dipolar couplings can make the dephasing curves of both moieties look similar, complicating the potential applications of the APT spectral editing to systems undergoing molecular motions such as synthetic and biopolymers.

Polarization transfer schemes offer an alternative route to spectral editing, which ends up alleviating both of these problems. Such methods constitute the basis of the standard sequences employed for liquid-state ^{13}C assignment purposes (INEPT, DEPT), and the well-defined dipolar evolution characterizing CH_n groups under moderately fast MAS experiments may enable their simple extension to the analysis of solids. An initial assay on the potential of these sequences was carried out by calculating the ^{13}C signals that will result from the action of the INEPT sequence

$$(\pi/2)_{^1H} - t_1^a - (\pi/2)_{^1H},\ (\pi/2)_{^{13}C} - t_1^b \qquad [2]$$

in the absence of ^{1}H,^{13}C chemical shift interactions. These experiments have in principle three variables that could help distinguish CH from CH_2 groups: t_1^a, t_1^b (with $0 \leq t_1^a, t_1^b \leq T_r$ as a result of the dipolar evolution's periodicity) and the effective ω_{CH}/ω_r ratio. If ^{1}H–^{1}H interactions are neglected, the polarization transfer function characterizing each type of group can be analytically calculated; for methines this will be given by the average over the (α, β, γ) powder angles of

$$S_{CH}(t_1^a, t_1^b) = \sin \int_0^{t_1^a} \omega_{CH}(t)dt \cdot \sin \int_{t_1^a}^{t_1^a+t_1^b} \omega_{CH}(t)dt, \qquad [3]$$

whereas for methylene groups CH_aH_b the transfer will arise from

$$S_{CH_2}(t_1^a, t_1^b) = \sin \int_0^{t_1^a} \omega_{CH_a}(t)dt \cdot \sin \int_{t_1^a}^{t_1^a+t_1^b} \omega_{CH_a}(t)dt \times \cos \int_{t_1^a}^{t_1^a+t_1^b} \omega_{CH_b}(t)dt. \qquad [4]$$

Figure 9 presents the powder-averaged intensities of these resulting signals as a function of t_1^a and t_1^b for a fixed $\omega_{CH}/2\pi =$ 21 kHz dipolar coupling and for various values of the ω_r rates. Also shown are the 2D maps that under these conditions could be calculated via complete propagations of the CH_2 groups that do not neglect homonuclear ^{1}H–^{1}H couplings. As in earlier examples, it is interesting to note that from a ^{13}C perspective

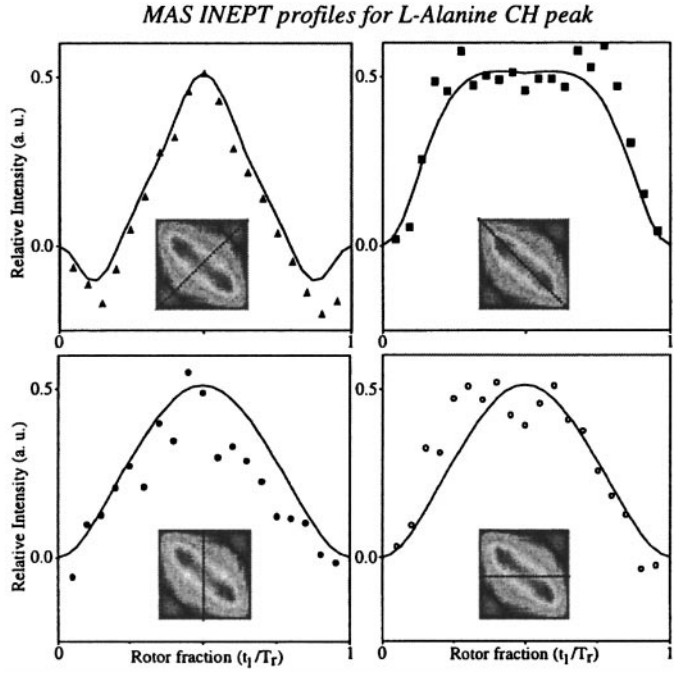

FIG. 10. Selected profiles observed for the solid-state INEPT transfer within L-alanine's CH group at $\omega_r/2\pi = 14$ kHz. The solid lines are simulations that assumed a ^{13}C–^{1}H coupling constant $\omega_{CH}/2\pi = 20.9$ kHz. The insets exemplify the slices shown by each plot within the context of the 2D $S(t_1^a, t_1^b)$ map.

and at the moderately fast spinning rates that are relevant for this study (>10 kHz), the main consequence of introducing these homonuclear ^{1}H–^{1}H couplings is a slight magnification of the apparent ω_{CH}/ω_r ratio.

When considering potential practical applications of these sequences, there are two regions in these 2D polarization-transfer maps that appear particularly interesting. One arises in the $\omega_r/2\pi \geq 20$ kHz fast-spinning regime, where setting $t_1^a \approx T_r/4$ and $t_1^b \approx 3T_r/4$ enables a coherent transfer of $^{1}H \rightarrow {}^{13}C$ polarization with relatively good efficiency (30–40%) for both methine and methylene groups. Given the challenges faced by CP sequences at such high spinning speeds, this could be useful for achieving an enhancement of the dilute spin signals.[4] The other regime of interest, relevant in the spectral editing scenario that is being here considered, arises when $\omega_r/2\pi \approx$ 6–8 kHz. Here the 2D $S(t_1^a, t_1^b)$ maps show that choosing $t_1^a = t_1^b = T_r/2$ can yield a polarization transfer of ≈60% for CH groups, while having a negligible efficiency in polarizing the CH_2 groups (regardless of whether ^{1}H–^{1}H couplings are taken into account). Furthermore, this selective polarization transfer is expected to occur over a relatively broad range of dipolar couplings, $0.3 \leq \omega_r/\omega_{CH} \leq 0.5$, thus reducing the editing's

[4] In fact, the potential of such coherence-transfer schemes in combination with even faster spinning rates and REDOR-driven recoupling has recently been exploited in the development of new solid-state HMQC experiments (*30*).

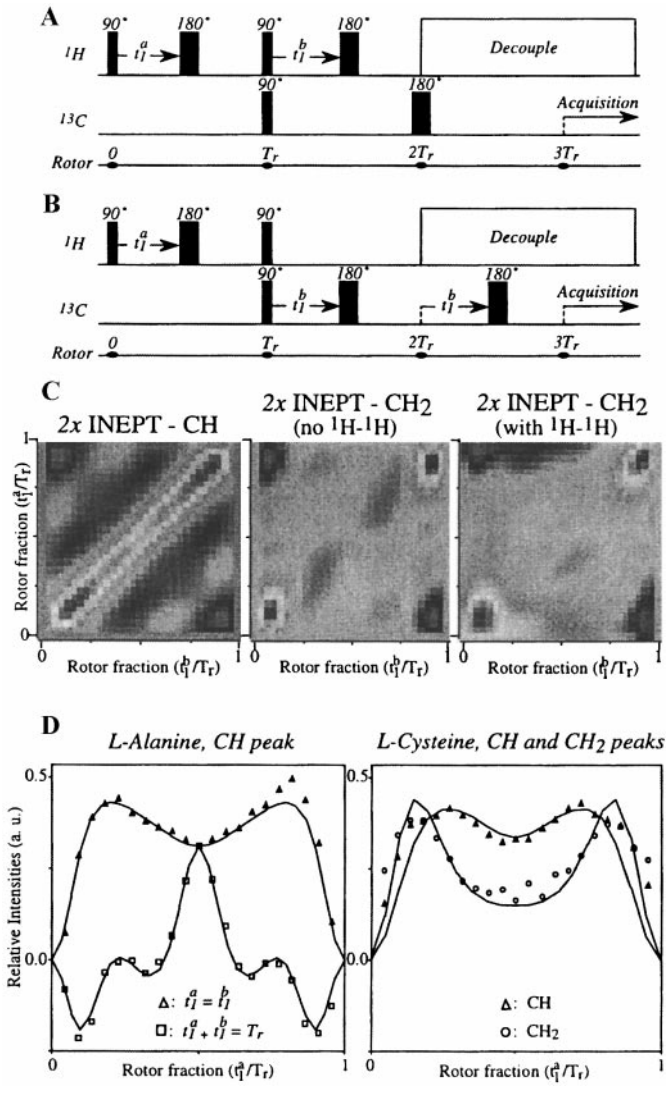

FIG. 11. (A, B) Pulse sequences explored in the implementation of 2*x*-INEPT editing. According to the maps in Fig. 9, methylene signals in these experiments should decay while all other carbons show up with their isotropic and anisotropic shifts refocused. (C) 2D maps resulting from the rigorous time propagation of sequence (A) for different CH_n models at $\omega_r/2\pi = 12$ kHz and for a ^{13}C–^1H coupling constant $\omega_{CH}/2\pi = 20.9$ kHz. Notice that, except for a reversal in the t_1^b evolution sense, there is a very good match between these maps and those calculated for the standard INEPT at half the spinning speed (Fig. 9, left column). (D) Comparisons between the expectations arising from these 2D $S(t_1^a, t_1^b)$ maps and experiments acquired on L-alanine and L-cysteine powders. Experimental 2*x*-INEPT data for L-alanine were collected at $\omega_r/2\pi = 14$ kHz for both the main (△) and the anti- (□) diagonal. Data for L-cysteine were acquired at $\omega_r/2\pi = 19$ kHz and are shown along the main diagonal for the CH (△) and the CH_2 peaks (○). The solid lines correspond to simulated curves.

sensitivity toward potential scaling effects of molecular motions.

As was the case for the various methods discussed earlier, we found that all of these predictions, particularly with regard to the absolute efficiencies expected from the polarization transfer processes, are best fulfilled when experiments are carried at moderately fast spinning rates (≥12 kHz). Examples of the good agreement which then results between these polarization-transfer expectations and experiments are illustrated in Fig. 10, which presents various $S(t_1^a, t_1^b)$ profiles for the CH group of alanine.

In order to exploit the dipolar editing possibilities opened up by these sequences, it is again convenient to carry out a 2*x* amplification of the ω_{CH}/ω_r ratio, as this allows one to mimic the spin evolution expected for $\omega_r \approx 6$–7 kHz while fulfilling moderately fast sample spinning conditions. Two experimental alternatives that combine INEPT coherence transfers, an effec-

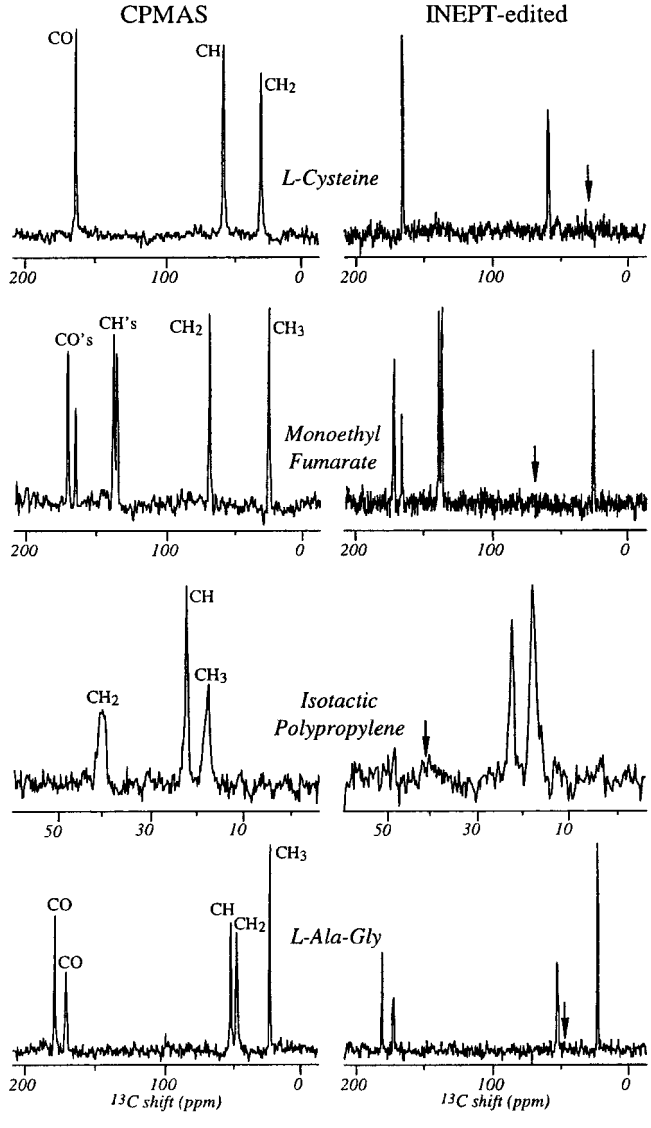

FIG. 12. Comparison between simple CPMAS (left) and 2*x*-INEPT-edited spectra (right column) acquired on a number of different organic compounds. Arrows in the latter indicate the positions of the missing methylene peaks.

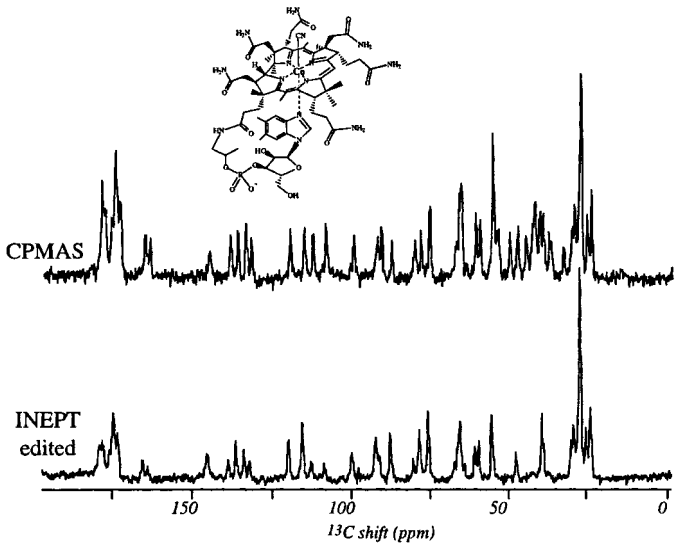

FIG. 13. Comparison between the CPMAS (2048 scans) and 2*x*-INEPT-edited (20,480 scans) spectra of vitamin B_{12}. A discussion on how these data facilitate the spectral assignment of the peaks is given in Ref. (*31*).

tive doubling of the ^1H–^{13}C local field couplings and an overall refocusing of the ^{13}C isotropic and anisotropic evolutions, are shown in Figs. 11A and 11B. The performances of these two sequences were found to be comparable, yet the version shown in Fig. 11A was preferred because of its slightly longer delay between the last ^{13}C pulse and the beginning of the signal acquisition. Numerical simulations then showed that apart for a scaling by a factor of 2 in the effective spinning rate and a reversal in the apparent sense of t_1^b evolution, the results which can be expected from this 2*x* INEPT sequence are very similar to those in the original $S(t_1^a, t_1^b)$ maps. Editing applications of such sequence to the identification of CH_2 resonances in a variety of organic compounds are illustrated in Figs. 12 and 13. In all cases the methylene removal is complete, while the average CH signal intensity is approximately half as large as expected from the numerical calculations (and ≈30% of the value observed under comparable CP conditions). Nonprotonated and methyl carbons, on the other hand, behave as weakly coupled methines and consequently lead to nonnegligible peak intensities in this kind of editing experiments.

4. DISCUSSION AND CONCLUSIONS

The purpose of this study was to explore the new opportunities that moderately fast MAS opens up toward the spectral editing of dilute spin-1/2 nuclei. At the center of these spectral editing protocols is the observation that if samples are spun at moderately fast MAS rates, ^1H–^1H multiple-pulse decoupling can be obviated when focusing on the short-term ^{13}C–^1H heteronuclear evolution. Simple π pulse manipulations can then be used to amplify the effective ω_{CH}/ω_r ratios, bringing them into a range where differences between the evolution of various CH_n groups are maximized and their simple discrimination enabled. The result is a new set of simple pulse sequences that can achieve spectral editing on a range of organic systems, with acceptable signal-to-noise and without requiring extensive tuneup procedures. Goals demonstrated for such sequences include an extension of the dipolar-dephasing approach to fast MAS rates, the application of CP/APT-type experiments to the assignment of methylene and methine resonances, and the use of polarization transfer schemes for achieving a clear CH/CH_2 discrimination with acceptable S/N and without resorting to CP. In all of the analyzed cases, the behavior observed experimentally correlated very well with theoretical expectations derived from numerical computations. Additional extensions of these principles are currently being explored.

ACKNOWLEDGMENTS

This work was supported by the National Science Foundation through Grants DMR-9806810 and CHE-9841790 (Creativity Extension Award). L.F. is a Camille Dreyfus Teacher–Scholar (1996–2001), University of Illinois Junior Scholar (1997–2000), and Alfred P. Sloan Fellow (1997–2000).

REFERENCES

1. A. Pines, M. G. Gibby, and J. S. Waugh, *J. Chem. Phys.* **59,** 569 (1973).
2. J. Schaefer and E. O. Stejskal, *J. Am. Chem. Soc.* **98,** 1031 (1976).
3. C. A. Fyfe, "Solid State NMR for Chemists," CFC Press, Ontario, 1983.
4. K. Schmidt-Rohr and H. W. Spiess, "Multidimensional Solid-State NMR and Polymers," Academic Press, New York, 1994.
5. A. E. Bennett, C. M. Rienstra, M. Auger, K. V. Lakshmi, and R. G. Griffin, *J. Chem. Phys.* **103,** 6951 (1995).
6. A. E. Derome, "Modern NMR Techniques for Chemistry Research," Pergamon Press, Oxford, 1987.
7. R. R. Ernst, G. Bodenhausen, and A. Wokaun, "Principles of Nuclear Magnetism in One and Two Dimensions," Oxford Univ. Press, London, 1987.
8. M. Alla and E. Lippmaa, *Chem. Phys. Lett.* **37,** 260 (1976).
9. S. J. Opella and M. H. Frey, *J. Am. Chem. Soc.* **101,** 5854 (1979).
10. T. Terao, H. Miura, and A. Saika, *J. Chem. Phys.* **75,** 1573 (1981).
11. T. Terao, H. Miura, and A. Saika, *J. Magn. Reson.* **49,** 365 (1982).
12. K. W. Zilm and D. M. Grant, *J. Magn. Reson.* **48,** 524 (1982).
13. G. G. Webb and K. W. Zilm, *J. Am. Chem. Soc.* **111,** 2455 (1989).
14. D. P. Burum and A. Bielecki, *J. Magn. Reson.* **95,** 184 (1991).
15. N. K. Sethi, *J. Magn. Reson.* **94,** 352 (1991).
16. X. Wu and K. W. Zilm, *J. Magn. Reson. A* **102,** 205 (1993).
17. X. Wu and K. W. Zilm, *J. Magn. Reson. A* **104,** 119 (1993).
18. R. Sangill, N. Rastrup-Andersen, H. Bildsøe, H. J. Jakobsen, and N. C. Nielsen, *J. Magn. Reson. A* **107,** 67 (1994).
19. X. Wu, S. T. Burns, and K. W. Zilm, *J. Magn. Reson. A* **111,** 29 (1994).

20. A. Lesage, C. Auger, S. Caldarelli, and L. Emsley, *J. Am. Chem. Soc.* **119,** 7867 (1997).

21. H. Pan, *J. Magn. Reson.* **124,** 1 (1997).

22. A. Lesage, S. Steuernagel, and L. Emsley, *J. Am. Chem. Soc.* **120,** 7095 (1998).

23. S. T. Burns, X. Wu, and K. W. Zilm, *J. Magn. Reson.* **143,** 352 (2000).

24. J. Z. Hu, J. K. Harper, C. Taylor, R. J. Pugmire, and D. M. Grant, *J. Magn. Reson.* **142,** 326 (2000).

25. D. McElheny, E. De Vita, and L. Frydman, *J. Magn. Reson.* **143,** 321 (2000).

26. O. B. Peersen, X. Wu, I. Kustanovich, and S. O. Smith, *J. Magn. Reson. A* **104,** 334 (1993).

27. M. Hong, J. D. Gross, and R. G. Griffin, *J. Phys. Chem. B* **101,** 5869 (1997).

28. M. Hong, J. D. Gross, C. M. Rienstra, R. G. Griffin, K. K. Kumashiro, and K. Schmidt-Rohr, *J. Magn. Reson.* **129,** 85 (1997).

29. P. Hodgkinson and L. Emsley, *J. Chem. Phys.* **107,** 4808 (1997).

30. K. Saalwächter, R. Graf, and H. W. Spiess, *J. Magn. Reson.* **140,** 471 (1999).

31. A. Medek and L. Frydman, *J. Am. Chem. Soc.* **122,** 684 (2000).